bioRxiv preprint doi: https://doi.org/10.1101/2021.02.09.430516; this version posted February 10, 2021. The copyright holder for this preprint (which was not certified by peer review) is the author/funder. All rights reserved. No reuse allowed without permission.

Development of a Triazolobenzodiazepine-Based PET Probe for Subtype-Selective Vasopressin 1A Receptor Imaging

Ahmed Haider[a⸸], Zhiwei Xiao [a⸸], Xiaotian Xia[a,b⸸], Jiahui Chen[a], Richard S. Van [c], Shi Kuang[d], Chunyu Zhao[a], Jian Rong[a], Tuo Shao[a], Perla Ramesh[e], Appu Aravind[e], Yihan Shao [c], Chongzhao Ran[d], Larry J. Young[f, g] and Steven H. Liang[a]*

[a] Department of Radiology, Division of Nuclear Medicine and Molecular Imaging Massachusetts General Hospital and Harvard Medical School, 55 Fruit Street, Boston, Massachusetts 02114, United States, E-mail: liang.steven@mgh.harvard.edu

[b] Department of Nuclear Medicine, Union Hospital, Tongji Medical College, Huazhong University of Science and Technology, Wuhan, 430022, China

[c] Department of Chemistry and Biochemistry, University of Oklahoma, Norman, OK 73019, United States

[d] Athinoula A. Martinos Center for Biomedical Imaging, Massachusetts General Hospital and Harvard Medical School, Boston, MA 02129, USA

[e] Sambi Pharma Pvt. Ltd., Hyderabad-500060, India

[f] Silvio O. Conte Center for Oxytocin and Social Cognition, Center for Translational Social Neuroscience, Yerkes National Primate Research Center, Emory University, Atlanta, GA, United States

[g] Department of Psychiatry and Behavioral Sciences, Emory University School of Medicine, Atlanta, GA, United Stated

⸸ Authors contributed equally to the work

bioRxiv preprint doi: https://doi.org/10.1101/2021.02.09.430516; this version posted February 10, 2021. The copyright holder for this preprint (which was not certified by peer review) is the author/funder. All rights reserved. No reuse allowed without permission.

Abstract

Objectives: Vasopressin 1A (V1A) receptors have been linked to autism spectrum disorder, heart failure, diabetes and renal disease. Currently, there is a lack of validated probes for clinical V1A-targeted imaging and previous PET studies have primarily focused on the brain. To enable non-invasive real-time quantification of V1A receptors in peripheral organs, we sought to develop a suitable PET radioligand that would allow specific and selective V1A receptor imaging *in vivo*.

Methods: The previously reported triazolobenzodiazepine-based V1A antagonist, PF-184563, served as a structural basis for the development of a suitable V1A-targeted PET probe. Initially, PF-184563 and the respective desmethyl precursor for radiolabeling were synthesized via multistep organic synthesis. Inhibitory constants of PF-184563 for V1A, V1B, V2 and oxytocin (OT) receptors were assessed by competitive radioligand binding or fluorescent-based assays. Molecular docking of PF-184563 to the V1A receptor binding pocket was performed to corroborate the high binding affinity, while carbon-11 labeling was accomplished via radiomethylation. To assess the utility of the resulting PET radioligand, [^{11}C]**17**, cell uptake studies were performed in a human V1A receptor Chinese hamster ovary (CHO) cell line under baseline and blockade conditions, using a series of V1A, V1B and V2 antagonists in >100-fold excess. Further, to show *in vivo* specificity, we conducted PET imaging and biodistribution experiments, thereby co-administering the clinical V1A-antagonist, balovaptan (3mg/kg), as a blocking agent.

Results: PF-184563 and the respective desmethyl precursor were synthesized in an overall yield of 49% (over 7 steps) and 40% (over 8 steps), respectively. A subnanomolar inhibitory constant (K_i) of 0.9 nM towards the V1A receptor was observed for PF-184563, while the triazolobenzodiazepine derivative concurrently exhibited excellent selectivity over the related V1B, V2 and OT receptor (IC_{50} >10,000 nM). [^{11}C]**17** was obtained in high radiochemical purity (> 99%), molar activities ranging from 37 - 46 GBq/µmol and a non-decay-corrected radiochemical yield of 8%. Cell uptake studies revealed considerable tracer binding, which was significantly reduced in the presence of V1A antagonists. Conversely, there was no significant blockade in the presence of V1B and V2 antagonists. PET imaging and biodistribution studies in CD-1 mice indicated specific tracer binding in the thyroid, pancreas, spleen and the heart.

Conclusion: We report the development of a V1A-targeted PET radioligand that is suitable for subtype-selective *in vitro* and *in vivo* receptor imaging. Indeed, [^{11}C]**17** proved to specifically visualize V1A receptors in several organs including the heart, pancreas, spleen and thyroid. These results suggest that [^{11}C]**17** can be a valuable tool to study the role of V1A receptors in cardiovascular and immune-mediated pathologies.

bioRxiv preprint doi: https://doi.org/10.1101/2021.02.09.430516; this version posted February 10, 2021. The copyright holder for this preprint (which was not certified by peer review) is the author/funder. All rights reserved. No reuse allowed without permission.

Key words: Vasopressin 1A receptor, pharmacology, positron emission tomography, tracer development, triazolobenzodiazepines

Introduction

Vasopressin 1A (V1A) receptors are transmembrane proteins that belong to the superfamily of G-protein-coupled receptors (GPCRs). [1] Notably, V1A receptor activation is triggered by an endogenous nonapeptide, arginine vasopressin (AVP), which is released from the posterior pituitary gland into the blood stream. [2, 3] Previous studies revealed that V1A receptors are expressed in the cardiovascular system, liver, kidney, pancreas, spleen, adipose tissue and the central nervous system (CNS). [4-6] Given the emerging focus on the role of V1A receptors in neurological pathologies, a plethora of studies outlined their distinct distribution in brain sections of different species.[7-9] Despite 83% of structural homology between rat and human V1A receptors, studies have unveiled substantial species-differences in the N-terminal domain that is involved in ligand binding. [10 11] To this end, significant species-dependent variability has been observed for the binding affinities of several synthetic V1A ligands.

V1A receptors have been initially been linked to autism spectrum disorder (ASD) [12, 13], Huntington's disease [14, 15], cerebral vasospasm [4] and brain edema [16], primary aldosteronism [17] and dysmenorrhea [18]. As such, strenuous drug discovery efforts led to the discovery of several potent antagonists, of which some have entered the clinical arena (**Figure 1**). YM471 was identified as a potent and long-acting V1A antagonist in rats, rendering it a useful tool to further elucidate the physiological and pathophysiological roles of V1A receptors. [19] Later, Guillon et. al reported on SRX246 and SRX251 as novel orally active V1A antagonists with subnanomolar affinities and CNS activity. As such, oral dosing of SRX246 and SRX251 led to brain levels that were ~100-fold higher than the respective inhibitory constants (K_i values). [20] Notwithstanding the potent anxiolytic effects of another ligand, JNJ-17308616, in preclinical experiments, as well as the high binding affinities towards both human and rat V1A receptors, no clinical studies with JNJ-17308616 have been reported to date. [21] Another potent V1A antagonist, YM218, exhibited a Ki value of 0.18 nM and has proven to attenuate vasopressin-induced growth responses of human mesangial cells. Accordingly, YM218 was suggested as a potential tool for investigating the role of V1A in the development of renal disease.[22, 23] As for the clinically tested candidates, relcovaptan (SR49059) showed favorable effects in patients with dysmenorrhea [24] and primary aldosteronism. [17, 25] Further, SRX246 was tested for the treatment of Huntington disease in a clinical phase II study. [14, 15] A CNS-targeted V1A antagonist, RG7713, exhibited beneficial effects in the treatment of abnormal affective speech recognition, olfactory identification and social communication in adult ASD

bioRxiv preprint doi: https://doi.org/10.1101/2021.02.09.430516; this version posted February 10, 2021. The copyright holder for this preprint (which was not certified by peer review) is the author/funder. All rights reserved. No reuse allowed without permission.

patients. [26] Further, the triazolobenzodiazepine, balovaptan (RG7314) showed encouraging results for the treatment of ASD in a clinical phase II study, which led to a Breakthrough Therapy Designation by the U.S. FDA in January 2018. [27] Despite these encouraging preclinical findings, the potential of V1A antagonists for the treatment of cardiovascular and immune-mediated diseases is largely unexplored. This has, at least in part, been attributed to the lack of appropriate tools for *in vivo* imaging of V1A receptors in peripheral organs.

Positron emission tomography (PET) is a powerful non-invasive imaging modality that allows real-time quantification of biochemical processes. Accordingly, PET has been established as a reliable tool for receptor quantification in preclinical and clinical research [28]. Further, it has proven particularly useful in facilitating drug discovery via target engagement studies [29, 30]. *In vivo* imaging and quantification of V1A receptors in the CNS as well as in peripheral organs is crucial to advance our understanding on the versatility of V1A receptor-related pathologies. Nonetheless, the development of a suitable PET radioligand remains challenging, and a clinically validated probe is currently lacking. To address this unmet medical need, radiolabeled analogues of SRX246 were synthesized, however, in vivo studies with these probes have not been reported, potentially owing to the relatively high molecular weight (700-800 Dalton) of this class of compounds – a feature that is known to hamper tracer pharmacokinetics. [31] Naik et al. recently reported on the development of [$^{11}CH_3$]*(1S,5R)*-**1**, a V1A-targeted PET ligand with subnanomolar biding affinity that was evaluated in rodents. [32] Despite the overall low brain uptake, specific in vivo binding was observed in the lateral septum of CD-1 mice. Further studies are warranted to assess whether sufficient brain exposure can be achieved with [$^{11}CH_3$]*(1S,5R)*-**1** to detect alterations in V1A receptor density in the CNS. While previous PET studies have exclusively focused on imaging V1A receptors in the CNS, there is a rapidly growing body of evidence suggesting that V1A receptors are implicated in serious peripheral pathologies including heart failure [33], diabetes [34], Raynaud's disease [33], gastric ulcers [35] and renal disease [22, 23]. Accordingly, we sought to develop a suitable V1A-targeted PET probe that would allow quantitative *in vivo* visualization of V1A receptors in peripheral organs such as the heart, kidney, pancreas and the spleen. Along this line, the previously reported triazolobenzodiazepine, PF-184563, was selected for radiolabeling and biological evaluation based on the subnanomolar binding affinity and the appropriate lipophilicity [36]. In the present study, we performed pharmacological profiling of PF-184563, conducted molecular docking studies, and evaluated the radiolabeled analog, [^{11}C]PF-184563, by cell uptake studies, *ex vivo* biodistribution experiments and PET imaging in rodents.

bioRxiv preprint doi: https://doi.org/10.1101/2021.02.09.430516; this version posted February 10, 2021. The copyright holder for this preprint (which was not certified by peer review) is the author/funder. All rights reserved. No reuse allowed without permission.

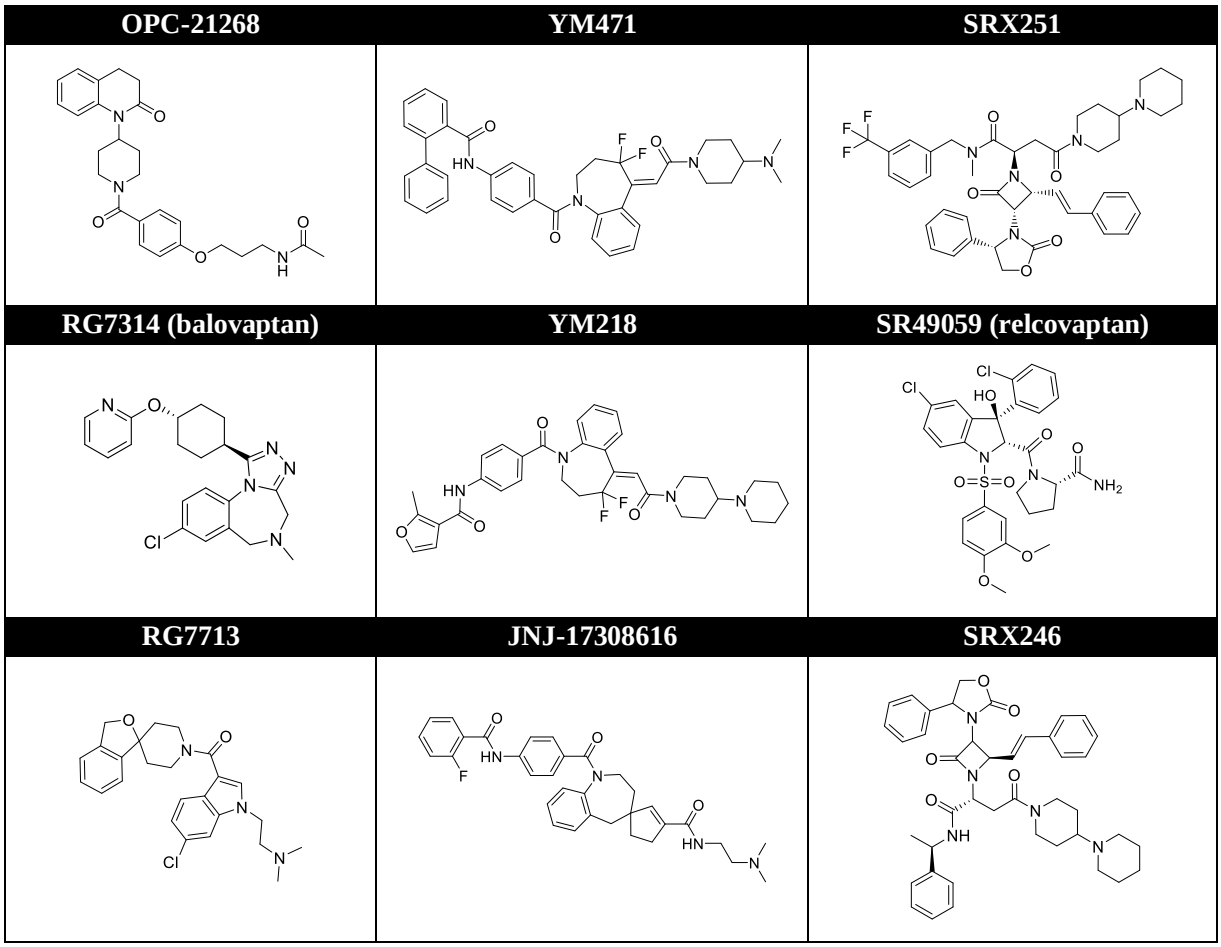

Figure 1. Selected Vasopressin 1A (V1A) receptor antagonists.

Results and Discussion

Chemical synthesis

Target compound **17** (PF-184563) and the respective desmethyl precursor **19** were synthesized as previously reported [36], however, with notable differences as outlined in **Schemes 1** and **2**. Indeed, the adapted synthetic strategy provided a common route for key intermediates **11** and **12** (**Scheme 1**), that were used for the synthesis of reference compound **17** and desmethyl precursor **19**, respectively, as depicted in **Scheme 2**. Further, this approach led to a ~ 3-fold increase of the overall yield for the synthesis of PF-184563, as compared to the previous report [36]. Briefly, commercially available benzyl alcohol **1** was chlorinated using sulfuryl chloride and the resulting intermediate **2** was employed in an N-alkylation reaction that afforded amines **3** and **4** in 90-99% yield. Subsequently, N-alkylation of **3** with ethyl bromoacetate in the presence of DIPEA yielded **5** in 93%, while amine protection of **4** with Boc anhydride afforded ester **6** in 78% yield. Reduction

bioRxiv preprint doi: https://doi.org/10.1101/2021.02.09.430516; this version posted February 10, 2021. The copyright holder for this preprint (which was not certified by peer review) is the author/funder. All rights reserved. No reuse allowed without permission.

of the nitro functionality was followed by an intramolecular amidation, which ultimately led to the formation of the benzodiazepine core structures in **9** and **10**, respectively. Key intermediates **11** and **12** were produced via thiation of the carbonyl group using the Lawesson's reagent.

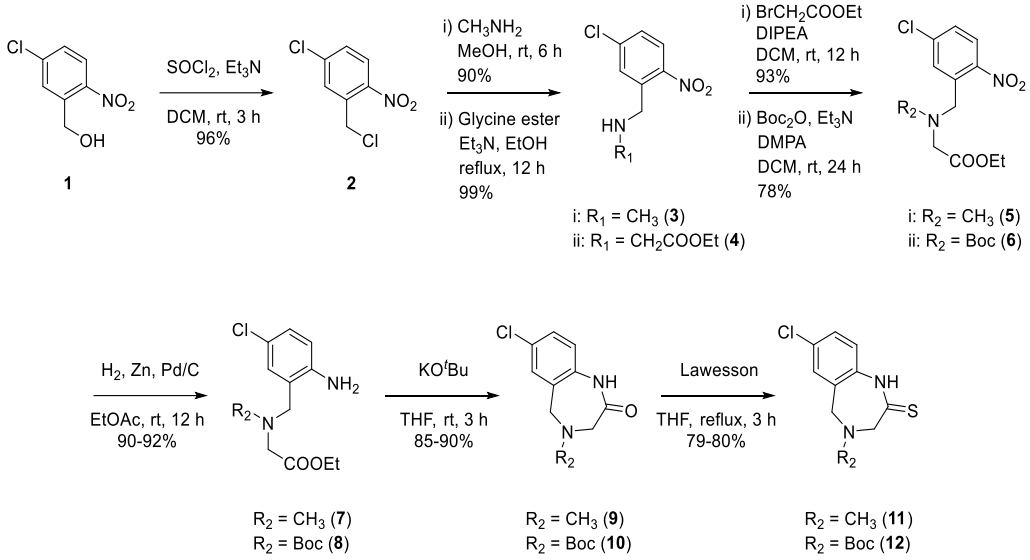

Scheme 1. Synthesis of key intermediates **11** and **12**.

Starting from commercially available 3-chloropyridine and ethyl piperidine-4-carboxylate, hydrazine **16** (**Scheme 2**) was synthesized in 83% yield over two steps. The 1,2,4-triazole analogues, reference compound **17** (PF-184563) and intermediate **18**, were prepared by intramolecular cyclization in refluxing n-butanol. Deprotection of **18** under acidic condition afforded precursor **19** in 81% yield. Overall, PF-184563 and the respective precursor **19** were synthesized in a yield of 49% (over 7 steps) and 40% (over 8 steps), respectively.

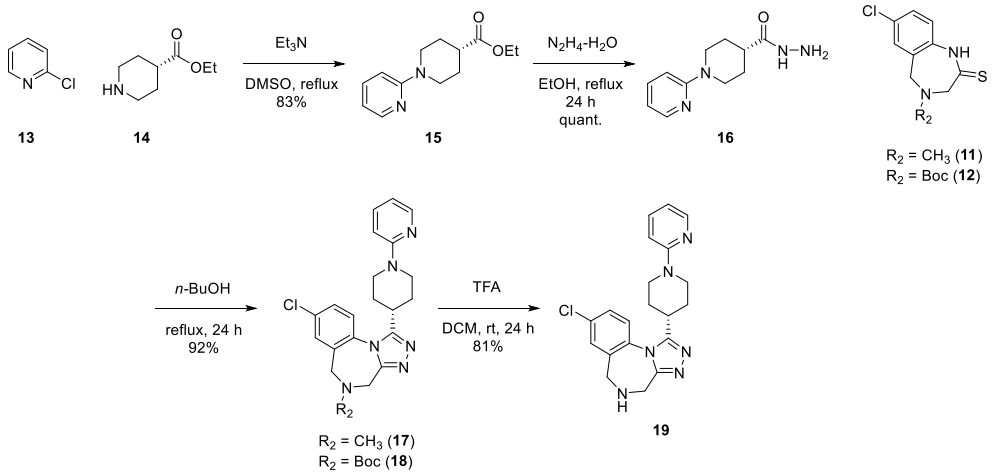

Scheme 2. Synthesis of target compound **17** (PF-184563) and precursor **19** for carbon-11 labeling.

bioRxiv preprint doi: https://doi.org/10.1101/2021.02.09.430516; this version posted February 10, 2021. The copyright holder for this preprint (which was not certified by peer review) is the author/funder. All rights reserved. No reuse allowed without permission.

Pharmacology Profiling

Pharmacological data of target compound **17** was assessed for the human V1A, V1B and V2 and OT, as well as for the hERG potassium channel, the L-type calcium channel and the sodium channel (**Figure 2**). In accordance with previous reports, **17** exhibited a high binding affinity (IC_{50} = 4.7 nM and K_i = 0.9 nM) towards the V1A receptor [36, 37]. Conversely, the binding affinities for related receptors, including V1B, V2 and oxytocin (OT) receptors, was >10 µM, suggesting a high compound selectivity. Similarly, **17** was deemed inactive against the hERG potassium channel, the L-type calcium channel and the sodium channel in concentrations up to 10 µM. These results confirmed that **17** exhibits high V1A affinity and selectivity.

	PF-184563
hV1A IC_{50} (nM)	4.7
hV1A K_i (nM)	0.9
hV1B IC_{50} (nM)	>10,000
hV2 IC_{50} (nM)	>10,000
hOT IC_{50} (nM)	>10,000
hERG channel	no inhibition at 10 µM
Calcium L-type channel	no inhibition at 10 µM
Sodium channel	no inhibition at 10 µM

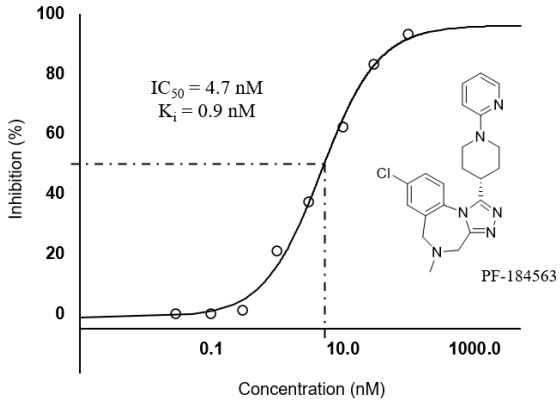

Figure 2. Summary of pharmacological properties for target compound **17** (PF-184563).

Molecular Docking

To rationalize the subnanomolar binding affinity, molecular interactions of PF-184563 with the V1A receptor were modeled using in silico simulations, as previously reported [38-40]. Since no crystal/NMR structures are available for the V1A receptor, an active state V1A homology model on gpcrdb.org was adopted and subsequently optimized via restrained energy minimization. Various compounds were docked to the V1A binding pocket of the homology model, which is composed of hydrophobic residues such as V100, M135, W304, and F307 (**Figure 3**). In the docking pose shown in **Figure 4**, the chlorine atom of PF-184563 was found to be in close proximity to the carbonyl groups of T333 (3.115 Å) and C303 (3.025 Å). Similarly, the triazole moiety was near Q131, with the closest distance between the amide hydrogen of Q131 and triazole nitrogens being 2.76 Å.

bioRxiv preprint doi: https://doi.org/10.1101/2021.02.09.430516; this version posted February 10, 2021. The copyright holder for this preprint (which was not certified by peer review) is the author/funder. All rights reserved. No reuse allowed without permission.

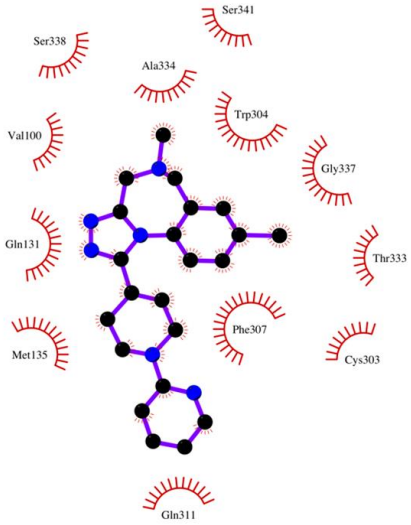

Figure 3. 2-D representation of protein-ligand complex of compound **17** (PF-184563) with the V1A receptor, as generated by LIGPLOT.

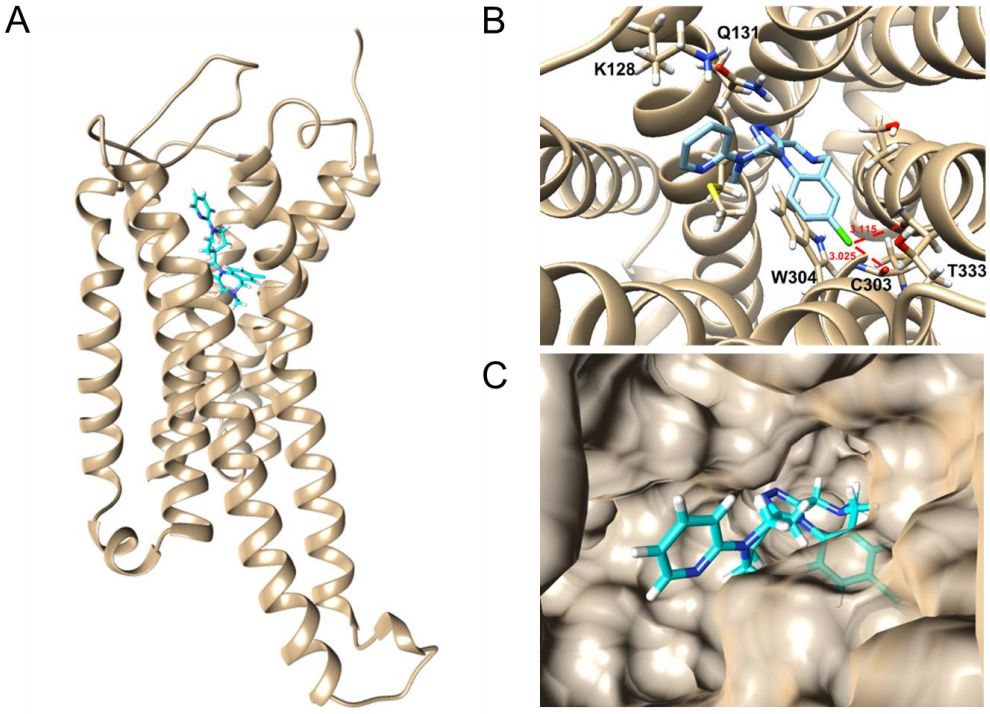

Figure 4. Molecular docking of PF-184563 to the V1A receptor. (**A**) Proposed binding site of the V1A receptor. (**B**) Predicted binding conformation of PF-184563 at the binding site. Residues within 3 Å are shown, with the distance of the chlorine atom with the carbonyls of C303 and T333 highlighted in red. (**C**) Surface representation of the binding pocket.

bioRxiv preprint doi: https://doi.org/10.1101/2021.02.09.430516; this version posted February 10, 2021. The copyright holder for this preprint (which was not certified by peer review) is the author/funder. All rights reserved. No reuse allowed without permission.

Radiochemistry

As depicted in **Figure 5A**, the amino group of precursor **19** was amenable for conventional carbon-11 labeling with [^{11}C]CH_3I, thus providing the radiolabeled analog, [^{11}C]**17**, in excellent radiochemical purity (> 99%) and molar activities ranging from 37 - 46 GBq/µmol. [^{11}C]**17** was synthesized with an automated module sequence that constituted radiolabeling, purification and formulation, with an overall synthesis time of 45 min. As expected, [^{11}C]**17** was stable in saline containing 10% EtOH, and no degradation was observed for up to 90 min. Employing the shake-flask method, a $logD_{7.4}$ of 2.13 ± 0.01 was determined.

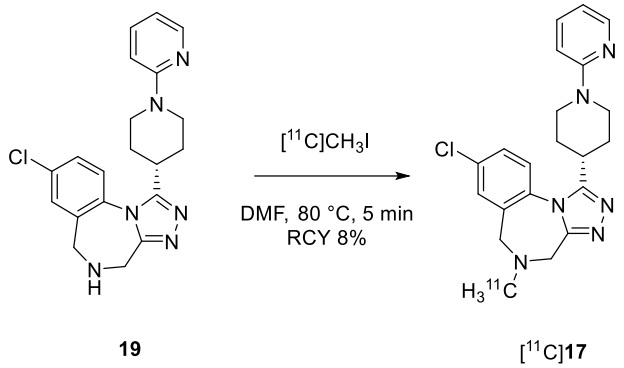

Figure 5. Radiosynthesis of [^{11}C]**17**. RCY, non-decay corrected radiochemical yield.

Cell uptake assay

Cell uptake assays were conducted in the presence of different inhibitors to demonstrate the specificity and selectivity of [^{11}C]**17** to the V1A receptor. As such, human V1A receptor-expressing Chinese hamster ovary (CHO) cells were seeded and incubated at 37 °C with either [^{11}C]**17** (**Figure 6**, control) or with a combination of [^{11}C]**17** and a >100-fold excess of the non-radioactive blockers, **17** (self-blocking), V1A antagonists, RG7713 and balovaptan, the V2 antagonists, mozavaptan and L-371,257, as well as the V1B antagonist, TASP 0390325). A significant reduction of [^{11}C]**17** cell uptake was observed under blockade conditions with all three V1A antagonists, while there was no significant blockade with mozavaptan, L-371,257 and TASP 0390325. These results indicate that [^{11}C]**17** specifically binds to the V1A receptor *in vitro*, thereby exhibiting appropriate selectivity over V1B and V2 receptors.

bioRxiv preprint doi: https://doi.org/10.1101/2021.02.09.430516; this version posted February 10, 2021. The copyright holder for this preprint (which was not certified by peer review) is the author/funder. All rights reserved. No reuse allowed without permission.

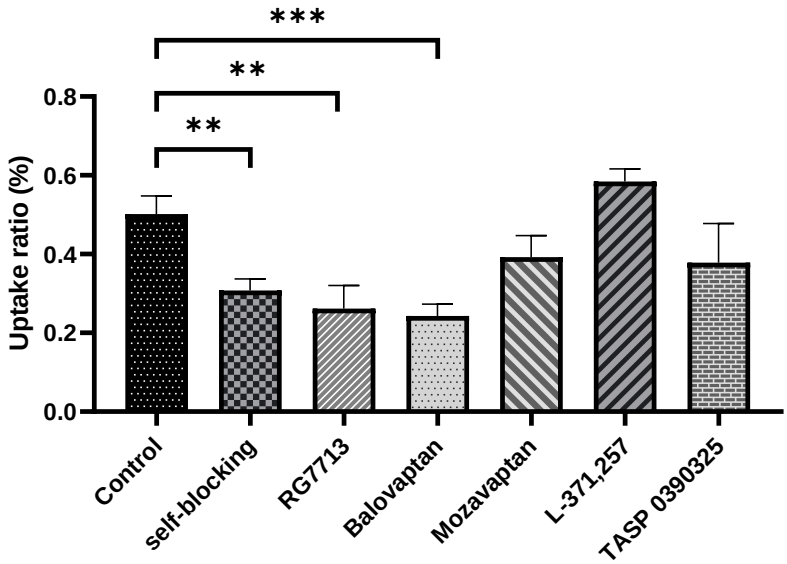

Figure 6. Uptake of [^{11}C]**17** in a human V1A receptor Chinese hamster ovary (CHO) cell line. Uptake was significantly reduced in the presence of non-radioactive 17, as well as the V1A receptor antagonists RG7713 and balovaptan. In contrast, no significant blocking effect was observed in the presence of mozavaptan (V2 receptor antagonist), L-371,257 (oxytocin receptor antagonist) and TASP 0390325 (V1B receptor antagonist). All blockers were used in a final assay concentration of 1 µM (>100-fold excess).

PET experiments

Dynamic PET scans were acquired following tail vein injection of [^{11}C]**17** in CD-1 mice. As such, representative sagittal and coronal PET images (summed 0–60 min) are depicted under baseline conditions (tracer only, **Figure 4A**). To assess specific binding of the tracer, the commercially available V1A antagonist, balovaptan (3 mg/kg), was administered 5 min prior to tracer injection (**Figure 4B**). In the baseline scan, the thyroid was clearly delineated, exhibiting an appropriate signal-to-back ratio and allowing quantitative PET (**Figure 4A,** right panel arrow**)**. Notably, the high tracer uptake in the thyroid was substantially reduced when balovaptan was co-administered (**Figure 4B,** right panel arrow**)**. Further, specific binding was observed in the abdominal cavity, however, given the combination of (1) the small size of the mouse, (2) the high density of abdominal organs with considerable tracer uptake and (3) the lack of computed tomography (CT) or magnetic resonance imaging (MRI) for anatomical orientation, we were not able to attribute the specific signal to abdominal organs based on the PET images. Therefore, ex vivo biodistributions studies were carried out.

bioRxiv preprint doi: https://doi.org/10.1101/2021.02.09.430516; this version posted February 10, 2021. The copyright holder for this preprint (which was not certified by peer review) is the author/funder. All rights reserved. No reuse allowed without permission.

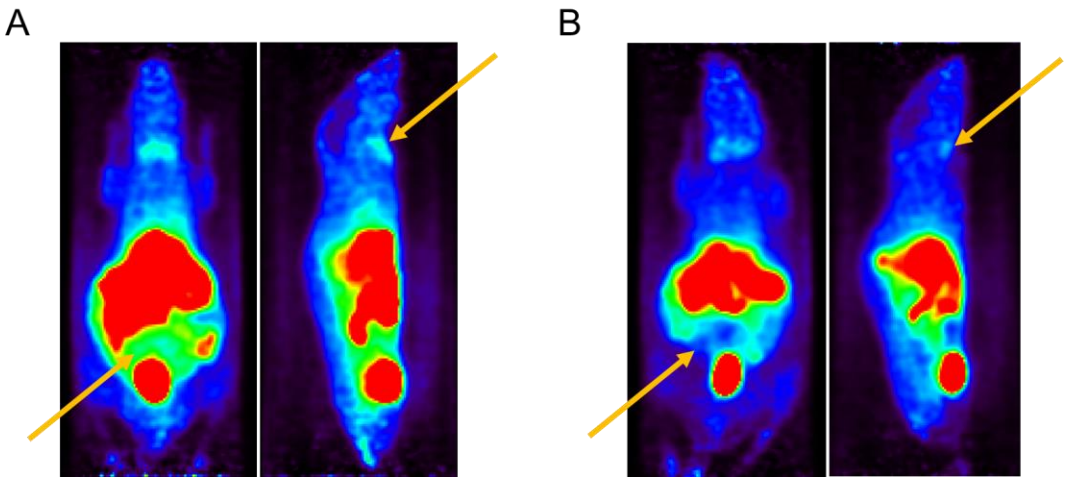

Figure 4. Representative PET images, following tail vein injection of [^{11}C]**17** in CD1 mice, averaged from 0-60 min post injection. (**A**) Coronal (left panel) and sagittal (right panel) images under baseline conditions, where only [^{11}C]**17** was injected. (**B**) Coronal (left panel) and sagittal (right panel) images under blocking conditions, where [^{11}C]**17** and V1A antagonist, balovaptan (3mg/kg), were injected. Arrows indicate successful blocking in the thyroid and abdominal organs.

Ex vivo biodistribution study

As previously mentioned, the delineation of abdominal organs by small-animal PET can be challenging. Accordingly, we sought to quantify the tracer uptake in a comprehensive set of organs by *ex vivo* biodistribution. Biodistribution data of [^{11}C]**17** were obtained in CD-1 mice at different time points (5, 15, 30 and 60 min) post injection. The data is presented as percentage of injected dose per gram tissue (**Figure 5A**, %ID/g). While the radioactivity uptake was generally high in the liver, kidney and small intestine, we observed a sustained accumulation with relatively slow washout – particularly at >15 min post injection – in the pancreas, thyroid, spleen and the heart, indicating that there might be specific binding in those organs. Next, we performed a blocking study with the clinical V1A antagonist, balovaptan, to confirm the specificity of the signal. Indeed, a significant signal reduction under blockade conditions was corroborated for the spleen, heart and pancreas, thus suggesting that [^{11}C]**17** specifically binds to V1A receptors *in vivo* (**Figure 6**).

bioRxiv preprint doi: https://doi.org/10.1101/2021.02.09.430516; this version posted February 10, 2021. The copyright holder for this preprint (which was not certified by peer review) is the author/funder. All rights reserved. No reuse allowed without permission.

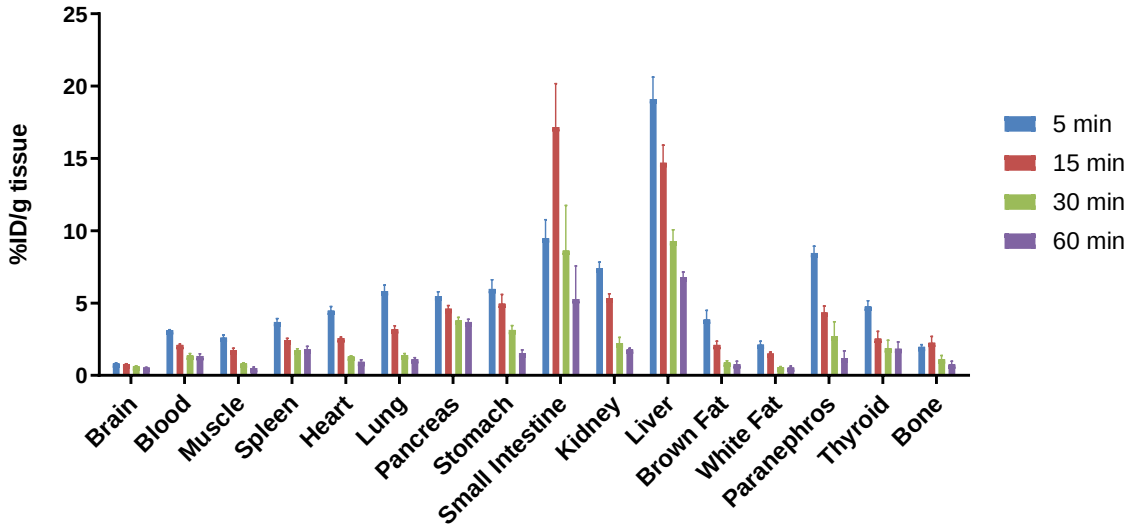

Figure 5. (A) *Ex vivo* whole body biodistribution in CD-1 mice at 5, 15, 30 and 60 min post injection of [^{11}C]**17**. The results are expressed as the percentage of the injected dose per gram tissue (% ID/g); All data are presented as mean ± standard error (SE), n = 4.

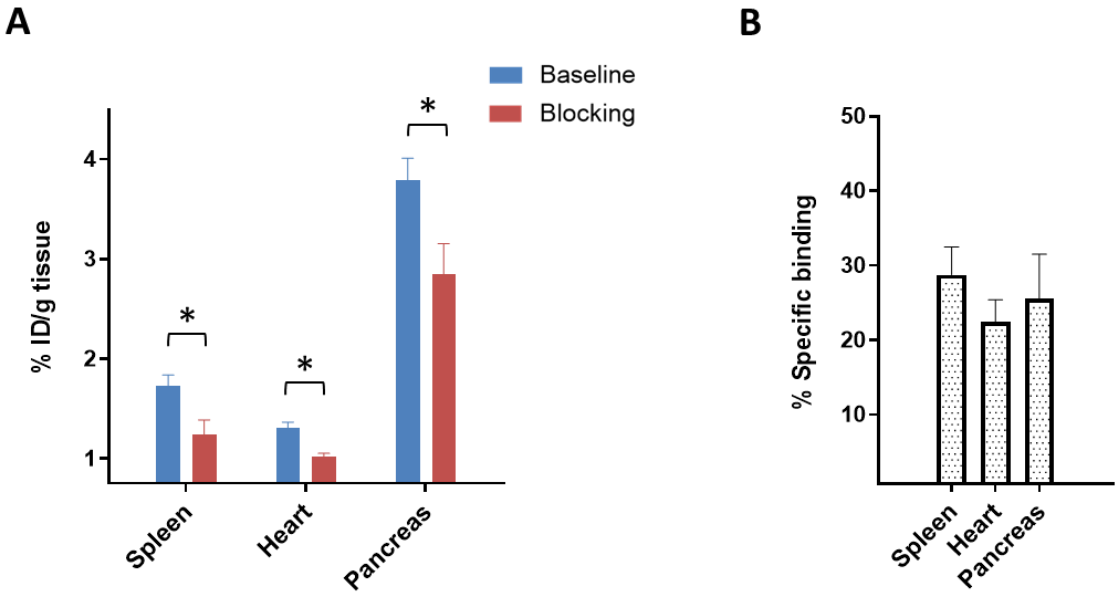

Figure 6. *Ex vivo* biodistribution in CD-1 mice under baseline and blockade conditions at 30 min post injection, with specificity in the spleen, heart and pancreas. Balovaptan (3 mg/kg) was used as a blocking agent. (**A**) Percentage of the injected dose per gram of wet tissue (% ID/g) under baseline and blocking conditions. A significant signal reduction was observed in the spleen, heart and pancreas. (**B**) Percentage of specific binding observed in each of the three organs. All data are mean ± standard error (SE), n = 4. Asterisks indicate statistical significance at $p < 0.05$.

bioRxiv preprint doi: https://doi.org/10.1101/2021.02.09.430516; this version posted February 10, 2021. The copyright holder for this preprint (which was not certified by peer review) is the author/funder. All rights reserved. No reuse allowed without permission.

Conclusion

A wealth of knowledge has been accumulated for the role of V1A receptors in peripheral pathologies such as heart failure, diabetes and renal disease. Further, there is preliminary evidence that V1A receptors are involved in B cell signaling [41]. Nonetheless, the role of V1A receptors in mediating immune functions is largely unexplored and there is a plethora of unanswered questions. To improve our understanding on how V1A receptor expression and function is affected in peripheral organs such as the heart, pancreas, spleen or kidney, a dedicated tool for non-invasive receptor visualization and quantification in patients is urgently needed. Of note, a clinically validated V1A-selective PET radioligand is currently lacking, and previous studies have exclusively focused on the development of CNS-targeted probes. To the best of our knowledge, this is the first report on a V1A PET radioligand that exhibits appropriate *in vitro* and *in vivo* specificity in peripheral organs, as evidenced by blockade studies in the heart, pancreas, thyroid and spleen. Our data suggests that [^{11}C]**17** harbors potential to enable selective V1A-targeted imaging and warrants further studies in animal models of cardiovascular and immune-mediated diseases. The availability of a clinical V1A-selective PET radioligand would facilitate drug development via target engagement studies and contribute to an improved understanding of the versatile roles of V1A receptors, ultimately resulting in an improved diagnostic care for the patient.

Acknowledgements

AH was supported by the Swiss National Science Foundation. LJY's contribution was supported by NIH grants P50MH100023 to LJY and P51OD11132 to YNPRC.

bioRxiv preprint doi: https://doi.org/10.1101/2021.02.09.430516; this version posted February 10, 2021. The copyright holder for this preprint (which was not certified by peer review) is the author/funder. All rights reserved. No reuse allowed without permission.

References

1. Barberis, C.; Mouillac, B.; Durroux, T. Structural bases of vasopressin/oxytocin receptor function. *The Journal of endocrinology* **1998,** 156, 223-9.
2. Holt, N. F.; Haspel, K. L. Vasopressin: a review of therapeutic applications. *Journal of cardiothoracic and vascular anesthesia* **2010,** 24, 330-47.
3. Hruby, V. J.; Chow, M. S.; Smith, D. D. Conformational and structural considerations in oxytocin-receptor binding and biological activity. *Annual review of pharmacology and toxicology* **1990,** 30, 501-34.
4. Koshimizu, T. A.; Nakamura, K.; Egashira, N.; Hiroyama, M.; Nonoguchi, H.; Tanoue, A. Vasopressin V1a and V1b receptors: from molecules to physiological systems. *Physiological reviews* **2012,** 92, 1813-64.
5. Barberis, C.; Audigier, S. [Vasopressin and oxytocin receptors in the central nervous system of the rat]. *Annales d'endocrinologie* **1985,** 46, 35-9.
6. Folny, V.; Raufaste, D.; Lukovic, L.; Pouzet, B.; Rochard, P.; Pascal, M.; Serradeil-Le Gal, C. Pancreatic vasopressin V1b receptors: characterization in In-R1-G9 cells and localization in human pancreas. *Am J Physiol Endocrinol Metab* **2003,** 285, E566-76.
7. Freeman, S. M.; Walum, H.; Inoue, K.; Smith, A. L.; Goodman, M. M.; Bales, K. L.; Young, L. J. Neuroanatomical distribution of oxytocin and vasopressin 1a receptors in the socially monogamous coppery titi monkey (Callicebus cupreus). *Neuroscience* **2014,** 273, 12-23.
8. Freeman, S. M.; Young, L. J. Comparative Perspectives on Oxytocin and Vasopressin Receptor Research in Rodents and Primates: Translational Implications. *Journal of neuroendocrinology* **2016,** 28.
9. Young, L. J.; Toloczko, D.; Insel, T. R. Localization of vasopressin (V1a) receptor binding and mRNA in the rhesus monkey brain. *Journal of neuroendocrinology* **1999,** 11, 291-7.
10. Tahara, A.; Tsukada, J.; Ishii, N.; Tomura, Y.; Wada, K.; Kusayama, T.; Yatsu, T.; Uchida, W.; Tanaka, A. Characterization of rodent liver and kidney AVP receptors: pharmacologic evidence for species differences. *Regulatory peptides* **1999,** 84, 13-9.
11. Pierce, M. L.; French, J. A.; Murray, T. F. Comparison of the pharmacological profiles of arginine vasopressin and oxytocin analogs at marmoset, macaque, and human vasopressin 1a receptor. *Biomedicine & Pharmacotherapy* **2020,** 126, 110060.
12. Wassink, T. H.; Piven, J.; Vieland, V. J.; Pietila, J.; Goedken, R. J.; Folstein, S. E.; Sheffield, V. C. Examination of AVPR1a as an autism susceptibility gene. *Molecular psychiatry* **2004,** 9, 968-72.
13. Tansey, K. E.; Hill, M. J.; Cochrane, L. E.; Gill, M.; Anney, R. J.; Gallagher, L. Functionality of promoter microsatellites of arginine vasopressin receptor 1A (AVPR1A): implications for autism. *Molecular autism* **2011,** 2, 3.
14. Fabio, K. M.; Guillon, C. D.; Lu, S. F.; Heindel, N. D.; Brownstein, M. J.; Lacey, C. J.; Garippa, C.; Simon, N. G. Pharmacokinetics and metabolism of SRX246: a potent and selective vasopressin 1a antagonist. *Journal of pharmaceutical sciences* **2013,** 102, 2033-2043.
15. Brownstein, M. J.; Simon, N. G.; Long, J. D.; Yankey, J.; Maibach, H. T.; Cudkowicz, M.; Coffey, C.; Conwit, R. A.; Lungu, C.; Anderson, K. E.; Hersch, S. M.; Ecklund, D. J.; Damiano, E. M.; Itzkowitz, D. E.; Lu, S.; Chase, M. K.; Shefner, J. M.; McGarry, A.; Thornell, B.; Gladden, C.; Costigan, M.; O'Suilleabhain, P.; Marshall, F. J.; Chesire, A. M.; Deritis, P.; Adams, J. L.; Hedera, P.; Lowen, K.; Rosas, H. D.; Hiller, A. L.; Quinn, J.; Keith, K.; Duker, A. P.; Gruenwald, C.; Molloy, A.; Jacob, C.; Factor, S.; Sperin, E.; Bega, D.; Brown, Z. R.; Seeberger, L. C.; Sung, V. W.; Benge, M.; Kostyk, S. K.; Daley, A. M.; Perlman, S.; Suski, V.; Conlon, P.; Barrett, M. J.; Lowenhaupt, S.; Quigg, M.; Perlmutter, J. S.; Wright, B. A.; Most, E.; Schwartz, G. J.; Lamb, J.; Chuang, R. S.; Singer, C.; Marder,

bioRxiv preprint doi: https://doi.org/10.1101/2021.02.09.430516; this version posted February 10, 2021. The copyright holder for this preprint (which was not certified by peer review) is the author/funder. All rights reserved. No reuse allowed without permission.

K.; Moran, J. A.; Singleton, J. R.; Zorn, M.; Wall, P. V.; Dubinsky, R. M.; Gray, C.; Drazinic, C. Safety and Tolerability of SRX246, a Vasopressin 1a Antagonist, in Irritable Huntington's Disease Patients-A Randomized Phase 2 Clinical Trial. *J Clin Med* **2020,** 9.

16. Manaenko, A.; Fathali, N.; Khatibi, N. H.; Lekic, T.; Hasegawa, Y.; Martin, R.; Tang, J.; Zhang, J. H. Arginine-vasopressin V1a receptor inhibition improves neurologic outcomes following an intracerebral hemorrhagic brain injury. *Neurochem Int* **2011,** 58, 542-548.

17. Perraudin, V.; Delarue, C.; Lefebvre, H.; Do Rego, J. L.; Vaudry, H.; Kuhn, J. M. Evidence for a role of vasopressin in the control of aldosterone secretion in primary aldosteronism: in vitro and in vivo studies. *J Clin Endocrinol Metab* **2006,** 91, 1566-72.

18. Liedman, R.; Grant, L.; Igidbashian, S.; James, I.; McLeod, A.; Skillern, L.; Akerlund, M. Intrauterine pressure, ischemia markers, and experienced pain during administration of a vasopressin V1a receptor antagonist in spontaneous and vasopressin-induced dysmenorrhea. *Acta Obstet Gynecol Scand* **2006,** 85, 207-11.

19. Tsukada, J.; Tahara, A.; Tomura, Y.; Wada, K.; Kusayama, T.; Ishii, N.; Aoki, M.; Yatsu, T.; Uchida, W.; Taniguchi, N.; Tanaka, A. Pharmacological characterization of YM471, a novel potent vasopressin V(1A) and V(2) receptor antagonist. *European journal of pharmacology* **2002,** 446, 129-38.

20. Guillon, C.; Koppel, G.; Brownstein, M.; Chaney, M.; Ferris, C.; Lu, S.-F.; Fabio, K.; Miller, M.; Heindel, N.; Hunden, D.; Cooper, R.; Kaldor, S.; Skelton, J.; Dressman, B.; Clay, M.; Steinberg, M.; Bruns, R.; Simon, N. Azetidinones as Vasopressin V1a Antagonists. *Bioorganic & medicinal chemistry* **2007,** 15, 2054-80.

21. Bleickardt, C. J.; Mullins, D. E.; Macsweeney, C. P.; Werner, B. J.; Pond, A. J.; Guzzi, M. F.; Martin, F. D.; Varty, G. B.; Hodgson, R. A. Characterization of the V1a antagonist, JNJ-17308616, in rodent models of anxiety-like behavior. *Psychopharmacology* **2009,** 202, 711-8.

22. Tahara, A.; Tsukada, J.; Tomura, Y.; Momose, K.; Suzuki, T.; Yatsu, T.; Shibasaki, M. Effects of YM218, a nonpeptide vasopressin V(1A) receptor-selective antagonist, on vasopressin-induced growth responses in human mesangial cells. *European journal of pharmacology* **2006,** 538, 32-8.

23. Tahara, A.; Tsukada, J.; Tomura, Y.; Suzuki, T.; Yatsu, T.; Shibasaki, M. Effect of YM218, a nonpeptide vasopressin V(1A) receptor-selective antagonist, on rat mesangial cell hyperplasia and hypertrophy. *Vascular pharmacology* **2007,** 46, 463-9.

24. Brouard, R.; Bossmar, T.; Fournié-Lloret, D.; Chassard, D.; Akerlund, M. Effect of SR49059, an orally active V1a vasopressin receptor antagonist, in the prevention of dysmenorrhoea. *Bjog* **2000,** 107, 614-9.

25. Steinwall, M.; Bossmar, T.; Brouard, R.; Laudanski, T.; Olofsson, P.; Urban, R.; Wolff, K.; Le-Fur, G.; Åkerlund, M. The effect of relcovaptan (SR 49059), an orally active vasopressin V1a receptor antagonist, on uterine contractions in preterm labor. *Gynecological Endocrinology* **2005,** 20, 104-109.

26. Umbricht, D.; Del Valle Rubido, M.; Hollander, E.; McCracken, J. T.; Shic, F.; Scahill, L.; Noeldeke, J.; Boak, L.; Khwaja, O.; Squassante, L.; Grundschober, C.; Kletzl, H.; Fontoura, P. A Single Dose, Randomized, Controlled Proof-Of-Mechanism Study of a Novel Vasopressin 1a Receptor Antagonist (RG7713) in High-Functioning Adults with Autism Spectrum Disorder. *Neuropsychopharmacology : official publication of the American College of Neuropsychopharmacology* **2017,** 42, 1924.

27. Schnider, P.; Bissantz, C.; Bruns, A.; Dolente, C.; Goetschi, E.; Jakob-Roetne, R.; Kunnecke, B.; Mueggler, T.; Muster, W.; Parrott, N.; Pinard, E.; Ratni, H.; Risterucci, C.; Rogers-Evans, M.; von Kienlin, M.; Grundschober, C. Discovery of Balovaptan, a Vasopressin 1a Receptor Antagonist for the Treatment of Autism Spectrum Disorder. *Journal of medicinal chemistry* **2020,** 63, 1511-1525.

bioRxiv preprint doi: https://doi.org/10.1101/2021.02.09.430516; this version posted February 10, 2021. The copyright holder for this preprint (which was not certified by peer review) is the author/funder. All rights reserved. No reuse allowed without permission.

28. Ametamey, S. M.; Honer, M.; Schubiger, P. A. Molecular imaging with PET. *Chem Rev* **2008,** 108, 1501-16.
29. Willmann, J. K.; van Bruggen, N.; Dinkelborg, L. M.; Gambhir, S. S. Molecular imaging in drug development. *Nature Reviews Drug Discovery* **2008,** 7, 591-607.
30. Rudin, M.; Weissleder, R. Molecular imaging in drug discovery and development. *Nat Rev Drug Discov* **2003,** 2, 123-31.
31. Fabio, K.; Guillon, C.; Lacey, C.; Lu, S.-F.; Heindel, N.; Ferris, C.; Placzek, M.; Jones, G.; Brownstein, M.; Simon, N. Synthesis and evaluation of potent and selective human V1a receptor antagonists as potential ligands for PET or SPECT imaging. *Bioorganic & medicinal chemistry* **2012,** 20, 1337-45.
32. Naik, R.; Valentine, H.; Hall, A.; Mathews, W. B.; Harris, J. C.; Carter, C. S.; Dannals, R. F.; Wong, D. F.; Horti, A. G. Development of a radioligand for imaging V(1a) vasopressin receptors with PET. *Eur J Med Chem* **2017,** 139, 644-656.
33. Lemmens-Gruber, R.; Kamyar, M. Vasopressin antagonists. *Cellular and Molecular Life Sciences* **2006,** 63, 1766.
34. Mohan, S.; Moffett, R. C.; Thomas, K. G.; Irwin, N.; Flatt, P. R. Vasopressin receptors in islets enhance glucose tolerance, pancreatic beta-cell secretory function, proliferation and survival. *Biochimie* **2019,** 158, 191-198.
35. Zelena, D.; Filaretova, L. Age-dependent role of vasopressin in susceptibility of gastric mucosa to indomethacin-induced injury. *Regulatory peptides* **2010,** 161, 15-21.
36. Johnson, P. S.; Ryckmans, T.; Bryans, J.; Beal, D. M.; Dack, K. N.; Feeder, N.; Harrison, A.; Lewis, M.; Mason, H. J.; Mills, J.; Newman, J.; Pasquinet, C.; Rawson, D. J.; Roberts, L. R.; Russell, R.; Spark, D.; Stobie, A.; Underwood, T. J.; Ward, R.; Wheeler, S. Discovery of PF-184563, a potent and selective V1a antagonist for the treatment of dysmenorrhoea. The influence of compound flexibility on microsomal stability. *Bioorganic & Medicinal Chemistry Letters* **2011,** 21, 5684-5687.
37. Baska, F.; Szántó, G.; Bozó, É.; Szakács, Z.; Dékány, M.; Szondiné Kordás, K.; Domány-Kovács, K.; Kurkó, D.; Hodoscsek, B.; Magdó, I.; Krámos, B.; Béni, Z.; Vastag, M.; Bata, I. Discovery of New Heterocyclic Ring Systems as Novel and Potent V1A Receptor Antagonists. *ACS Chemical Neuroscience* **2020,** 11, 3532-3540.
38. Trott, O.; Olson, A. J. AutoDock Vina: improving the speed and accuracy of docking with a new scoring function, efficient optimization, and multithreading. *J Comput Chem* **2010,** 31, 455-461.
39. Pettersen, E. F.; Goddard, T. D.; Huang, C. C.; Couch, G. S.; Greenblatt, D. M.; Meng, E. C.; Ferrin, T. E. UCSF Chimera--a visualization system for exploratory research and analysis. *J Comput Chem* **2004,** 25, 1605-12.
40. D.A. Case, K. B., I.Y. Ben-Shalom, S.R. Brozell, D.S. Cerutti, T.E. Cheatham, III, V.W.D. Cruzeiro, T.A. Darden, R.E. Duke, G. Giambasu, M.K. Gilson, H. Gohlke, A.W. Goetz, R. Harris, S. Izadi, S.A. Izmailov, K. Kasavajhala, A. Kovalenko, R. Krasny, T. Kurtzman, T.S. Lee, S. LeGrand, P. Li, C. Lin, J. Liu, T. Luchko, R. Luo, V. Man, K.M. Merz, Y. Miao, O. Mikhailovskii, G. Monard, H. Nguyen, A. Onufriev, F.Pan, S. Pantano, R. Qi, D.R. Roe, A. Roitberg, C. Sagui, S. Schott-Verdugo, J. Shen, C. Simmerling, N.R.Skrynnikov, J. Smith, J. Swails, R.C. Walker, J. Wang, L. Wilson, R.M. Wolf, X. Wu, Y. Xiong, Y. Xue, D.M. York and P.A. Kollman. AMBER 2020. *University of California, San Francisco* **2020**.
41. Hu, S. B.; Zhao, Z. S.; Yhap, C.; Grinberg, A.; Huang, S. P.; Westphal, H.; Gold, P. Vasopressin receptor 1a-mediated negative regulation of B cell receptor signaling. *J Neuroimmunol* **2003,** 135, 72-81.